Materials Performance and Characterization

doi:10.1520/MPC20180079 / Vol. 7 / No. 1 / 2018 / available online at www.astm.org

Sunil Waddar,[1] Jeyaraj Pitchaimani,[2] Mrityunjay Doddamani,[1] and Nikhil Gupta[3]

Buckling and Free Vibration Behavior of Cenosphere/Epoxy Syntactic Foams under Axial Compressive Loading

Reference

Waddar, S., Pitchaimani, J., Doddamani, M., and Gupta, N., "Buckling and Free Vibration Behavior of Cenosphere/Epoxy Syntactic Foams under Axial Compressive Loading," *Materials Performance and Characterization*, Vol. 7, No. 1, 2018, pp. 532–546, https://doi.org/10.1520/MPC20180079. ISSN 2379-1365

ABSTRACT

The buckling and free vibration behavior of cenosphere/epoxy syntactic foams under axial compressive loading are investigated experimentally in this work. The buckling load is obtained from the load-deflection curve based on the Double Tangent Method (DTM) and Modified Budiansky Criteria (MBC). Furthermore, the influence of an axial compression load on the natural frequencies associated with the first three transverse bending modes is analyzed. Finally, the buckling loads predicted using DTM and MBC are compared to the buckling load calculated based on the vibration correlation technique. It is observed that the buckling loads predicted through the three different methods are in close agreement. The experimental results revealed that the buckling load and natural frequency of the syntactic foams increase with the cenosphere volume fraction. It is observed that the natural frequencies reduce with increases in the axial compression load for all the modes. However, a rapid increase in the fundamental frequency is observed when the compressive load is near and beyond the critical buckling load.

Keywords

fly ash cenospheres, syntactic foam, buckling, free vibration, axial compressive load

Manuscript received May 18, 2018; accepted for publication October 9, 2018; published online November 27, 2018.

[1] Department of Mechanical Engineering, National Institute of Technology Karnataka, Surathkal, Mangalore 575025, India

[2] Department of Mechanical Engineering, National Institute of Technology Karnataka, Surathkal, Mangalore 575025, India (Corresponding author), e-mail: pjeyaemkm@gmail.com, https://orcid.org/0000-0002-8456-8052

[3] Composite Materials and Mechanics Laboratory, Mechanical and Aerospace Engineering Department, Tandon School of Engineering, New York University, 6 MetroTech Center, Brooklyn, NY 11201, USA, https://orcid.org/0000-0001-7128-4459

Introduction

Polymer matrix composites offer a high specific strength and stiffness in weight-sensitive structures [1]. Syntactic foams are lightweight particulate composites with a wide variety of applications in marine, automotive, and aerospace structures [2]. These foams are synthesized by dispersing hollow particles in a matrix material. They are considered closed-cell structured foams with an excellent combination of compressive strength, low density, and damping behavior [2,3], which is promising for automotive and aerospace applications. Many of the structural components are slender in order to keep the structural weight low. These long and slender structures can be subjected to compressive loads during their service life, resulting in buckling failure. Hence, these applications also require understanding the buckling and dynamic behavior of structures made of syntactic foams under axial compressive load for improved designs.

Structure–property correlations for syntactic foams and different approaches for tailoring their properties have been extensively studied in the available literature [4–7]. Gupta, Woldesenbet, and Mensah [6] studied the effect of the hollow particle radius and specimen aspect ratio on the compressive behavior of cenosphere/epoxy syntactic foam. The results reveal that with a decrease in the internal radius of the cenosphere particle modulus, the compressive strength increases. Doddamani et al. [8] studied the flexural and compressive properties of plain and functionally graded cenosphere/epoxy foams. They observed that increasing the filler content increases the specific flexural modulus and strength. The mechanical and thermal properties of fly ash cenosphere, reinforced in a vinyl ester matrix, are studied by Labella et al. [9]; they observed that the stiffness of the composite increased with an increase in the filler content with enhanced dimensional stability. A significant amount of work has been done on the mechanical characterization of polymer matrix syntactic foams [6,10,11], but studies on buckling behavior are scarce. Although the use of engineered glass microballoons is preferred for developing high-performance syntactic foams [12,13], fly ash cenospheres are being studied as an alternate, due to their lower cost [8]. Cenosphere-filled syntactic foams are studied in the present work for free vibration and buckling characteristics.

Shams, Aureli, and Porfiri investigated the nonlinear buckling of a spherical shell embedded in an elastic medium under a uniaxial compressive load [14]. Numerical investigations revealed that the failure of syntactic foam is not governed by the microballoon shell buckling, but rather is governed by the shearing of the particle, as syntactic foams are fabricated with thin-walled particles to obtain a weight-saving advantage. The failure mechanism of cenosphere/epoxy syntactic foam subjected to compressive load was analyzed by Haung et al. [15] using finite element analysis. They found that the stress concentration in cenospheres is higher than in an epoxy matrix, making cenospheres the main load-bearing constituent. The results also showed that the failure occurs because of the cenospheres crushing and the plastic deformation of the epoxy matrix.

Buckling instabilities with axial stresses were investigated by Matsunaga [16,17], who observed good agreement between the Timoshenko beam theory and experimental results. Experiments on the buckling of polymer matrix composites have been addressed in Refs. [18,19]. Yang, Wu, and Kitipornchai [20] investigated the buckling and post-buckling of functional graded multilayer graphene platelet-reinforced composite beams based on the shear deformation theory showing a higher resistance with the addition of graphene platelet nanofillers.

Previous studies on metal matrix syntactic foams have shown that it is very difficult to extract reliable values of an elastic modulus from compression tests because of machine compliance issues. Free vibration-based dynamic characterization has been conducted on aluminum matrix syntactic foam core sandwiches [21,22] and was found to be successful in measuring the modulus of the composite. The influence of the specimen size and thickness and the volume fraction of the inclusions on the natural frequencies of a glass microballoon-epoxy syntactic foam sandwich with graphite-epoxy laminated skins revealed an increase in the natural frequencies with the filler volume fraction and wall thickness [23,24]. Rahmani et al. [25] investigated the free vibration response of sandwich beams with a functionally graded syntactic foam core based on the higher order sandwich theory. They found that the natural frequency of the sandwich beam increases with inhomogeneity (functional gradation) of the core material.

Owing to their higher specific properties, syntactic foams have the potential to replace conventional materials in marine, aerospace, and automobile applications in which the buckling and free vibration response of materials is relevant. Thus, the present work is focused on studying the buckling and free vibration response of fly ash cenosphere/epoxy syntactic foams. The experimental buckling loads are compared to the results obtained from the vibration correlation technique (VCT). Success in measuring the elastic properties of syntactic foams by the free vibration method can help in measuring the properties nondestructively, even for some of the parts that are in service. Finally, the fundamental frequency is estimated for the first three transverse free vibration modes, with respect to axial loading.

Materials and Methods

CONSTITUENT MATERIALS

Diglycidyl ether of bisphenol A–based epoxy resin, Lapox L-12, with a room-temperature curing polyamine K-6 hardener, supplied by Atul Ltd., Valsad, India, is used as the matrix resin. Fly ash cenospheres of grade CIL 150, supplied by Cenosphere India Pvt. Ltd., Kolkata, West Bengal, India, are used as the filler material. The chemical, physical, and sieve analysis of the cenospheres are presented in Table 1. The major constituents of the

TABLE 1

Physical, chemical, and sieve analysis details of cenospheres, as provided by the supplier.

Physical Properties		Chemical Analysis		Sieve Analysis	
True particle density	920 kg/m^3	SiO_2	52–62 %	+ 30 # (500 μm)	Nil
Bulk density	400–450 kg/m^3	Al_2O_3	32–36 %	+ 60 # (250 μm)	Nil
Hardness (MOH)	5–6	CaO	0.1–0.5 %	+ 100 # (150 μm)	Nil
Compressive strength	0.00176–0.00274 MPa	Fe_2O_3	1–3 %	+ 150 # (106 μm)	0–6 %
Shape	Spherical	TiO_2	0.8–1.3 %	+ 240 # (63 μm)	70–95 %
Packing factor	60–65 %	MgO	1–2.5 %	+ 240 #	0–30 %
Wall thickness	5–10 % of shell dia.	Na_2O	0.2–0.6 %	–	–
Color	Light gray – light buff	K_2O	1.2–3.2 %	–	–
Melting point	1,200–1,300°C	CO_2	70 %	–	–
pH in water	6–7	N_2	30 %	–	–
Moisture	0.5 % max.	–	–	–	–
Loss on ignition	2 % max.	–	–	–	–
Sinkers	5 % max.	–	–	–	–
Oil absorption	16–18 g/100 g	–	–	–	–

TABLE 2
Density of syntactic foams.

Material Type	Theoretical Density, kg/m^3	Experimental Density, kg/m^3	Matrix Void Content, %
E0	1,189.54	1,189.54 ± 0.04	–
E20	1,135.63	1,113.01 ± 3.56	1.99
E40	1,081.72	1,057.74 ± 6.48	2.22
E60	1,027.82	1,001.49 ± 9.54	2.56

cenospheres are silicon dioxide (SiO_2) and aluminum oxide (Al_2O_3), and the minor constituents are iron(III) oxide, calcium oxide, titanium dioxide, magnesium oxide, sodium oxide, and potassium monoxide. The density of the epoxy matrix is based on the experimental data (see Table 2), and the cenospheres' density is taken from the supplier data (see Table 1). Syntactic foams are fabricated with 20, 40, and 60 volume percent (vol.%) of cenospheres.

SYNTACTIC FOAM FABRICATION

The syntactic foam samples are prepared by manual stir mixing. The appropriate amount of cenospheres are weighed and mixed in the epoxy resin until a homogeneous slurry is obtained. Polymerization is initiated in the slurry by adding 10 weight percent of the hardener. The mixture is gently stirred again to mix the hardener homogeneously before pouring into an aluminum mold coated with a silicone releasing agent. After 24 hr of curing, cast slabs are removed and subjected to post-curing at 100°C for 3 hr. A diamond saw is used to section the samples to 310 by 12.5 by 4 mm^3 dimensions. All the samples are coded as per the nomenclature EXX, where 'E' denotes epoxy resin and 'XX' represents the cenosphere vol.%. For example, E40 refers to epoxy resin filled with 40 vol.% of cenospheres. The density of all the syntactic foams is measured as per the ASTM D792-13 standard, *Standard Test Methods for Density and Specific Gravity (Relative Density) of Plastics by Displacement*. The theoretical densities of the syntactic foams are estimated using the rule of mixtures. The difference between the experimental and theoretical densities is used to compute the void volume fraction (Φ_v) and is given by the following:

$$\Phi_v = \frac{\rho^{th} - \rho^{exp}}{\rho^{th}} \times 100 \quad (1)$$

where ρ^{th} and ρ^{exp} are the theoretical and experimental densities, respectively. This calculation underestimates the void content, because it assumes that no cenospheres are fractured during processing.

BUCKLING TEST

Syntactic foam specimens are subjected to axial compression in a universal testing machine (H75KS, Tinius Olsen, Salfords, Surrey, UK) with a load cell capacity of 50 kN to conduct the buckling test (see Fig. 1). Specimens are rigidly clamped in the grips on either end with 210 mm of free length to resemble the clamped-clamped condition. Five specimens of each composition are tested, and average values are reported. A crosshead displacement rate is maintained constant at 0.2 mm/min. Based on preliminary testing, the end shortening limit is set at 0.75 mm for all the tests to detect any post-buckling behavioral changes. The critical buckling load P_{cr} is determined graphically (see Fig. 2) from the experimentally acquired load-deflection data using the Double Tangent Method (DTM)

FIG. 1

Schematic experimental setup, showing buckling and free vibration tests.

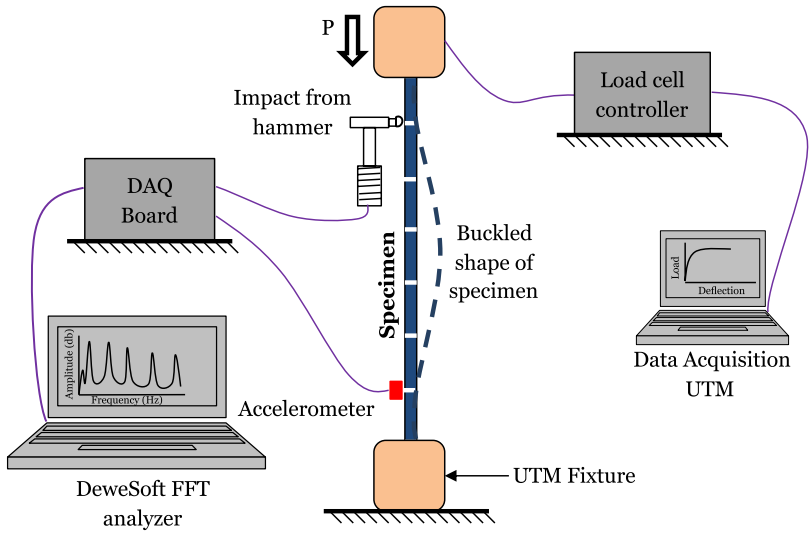

FIG. 2

Illustration of estimation of P_{cr} from experimental results using (a) DTM and (b) MBC methods.

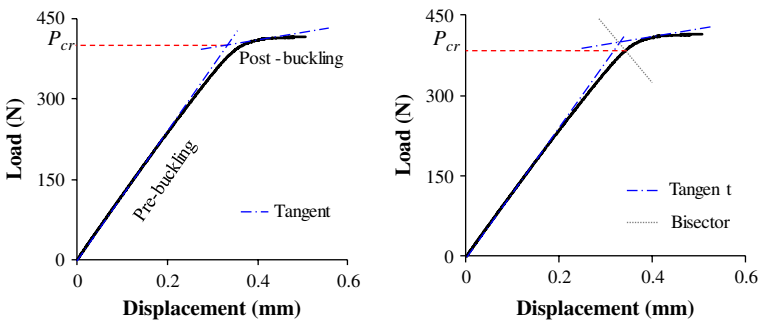

and Modified Budiansky Criteria (MBC) [26,27]. DTM is a two-tangents method in which tangents are drawn in the pre- and post-buckling regimes. The intersection point of the two tangents determines P_{cr}, as seen in Fig. 2a. In MBC, the load value corresponding to the bisector at the intersection points of both the tangents determines P_{cr} (see Fig. 2b). Results from both these methods are reported for comparative studies because of the lack of available literature on the buckling of syntactic foams.

FREE VIBRATION TEST

Experiments on modal analysis are conducted to obtain the first three natural frequencies with clamped-clamped boundary conditions under compressive load, as illustrated in Fig. 1. The roving hammer method is used to excite the specimen with a Kistler 9722A2000 impulse hammer (Kistler Group, Winterthur, Switzerland). Vibration signals are recorded by a Kistler 8778A500 uniaxial accelerometer (Kistler Group, Winterthur, Switzerland) with a measuring range of ±500 g, sensitivity of 9.60 mV/g, and resonant frequency of

76 kHz. DEWESoft modal analysis software (DEWESoft d.o.o., Trbovlje, Slovenia) is used to convert the time domain response to the frequency domain based on the fast Fourier transform algorithm. Furthermore, the natural frequency is estimated through the frequency response function and Nyquist plot, using the circle fit method. The test is carried out under no load condition and load increments of 50 N until the sample deflection reaches 0.75 mm. The test is paused for 2 minutes after each load increment, and modal analysis is performed to evaluate the natural frequencies in axial compression.

Free Vibration under No Load Condition

The experimentally measured natural frequencies of syntactic foams with no load conditions are compared to the analytical solutions given by Thomson, Dahleh, and Padmanabhan [28]. These analytical expressions are based on the Euler-Bernoulli hypothesis applied to homogenous materials. The random dispersion of spherical microparticles, such as cenospheres, is expected to result in a homogeneous material at the macroscale. Hence, analytical expressions for homogeneous materials can be used for syntactic foams. For bending, the angular natural frequency of the jth mode (ω_j) is given by [28] as follows:

$$\omega_j = \beta_j^2 \sqrt{\frac{EI}{\rho^{th} A L^4}} \tag{2}$$

where E is Young's modulus, I is the moment of inertia, L is the beam length (210 mm), and β is a constant (4.73, 7.8532, and 10.995 for the first, second, and third mode, respectively, for clamped-clamped boundary conditions [28]).

MICROGRAPHY

A JSM 6380LA scanning electron microscope (JEOL Ltd., Akishima, Tokyo, Japan) is used for microstructural analysis. All the samples are sputter coated using a JFC-1600 auto fine coater (JEOL Ltd., Akishima, Tokyo, Japan) prior to analysis.

Results and Discussions

Scanning electron micrographs of cenospheres are represented in Fig. 3. From Fig. 3a it can be observed that some of the cenospheres are not perfectly spherical, and some cenospheres have surface defects. Higher magnification of one such cenosphere (see Fig. 3b) shows porosity within the cenosphere shell and variation in the wall thickness. The

FIG. 3

Scanning electron micrographs of (a) cenosphere particles and (b) wall thickness variations and in-built porosity present in cenospheres.

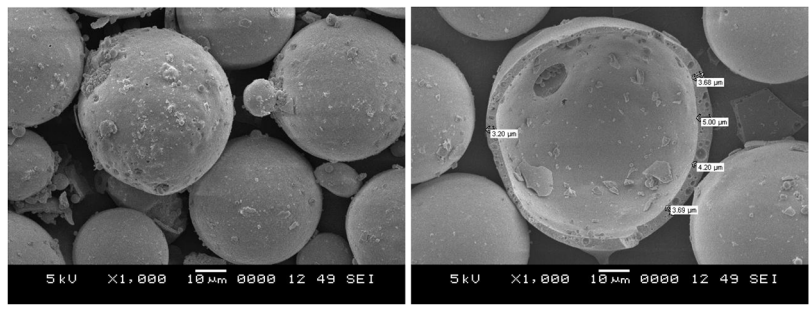

(a) (b)

presence of porosity in the walls results in a reduction in the mechanical properties of these particles compared to their expected value. In the present study, manual stir mixing is employed to prepare cenosphere/epoxy syntactic foams. The high quality of the samples depends on the uniform distribution of cenospheres, lack of agglomeration, and minimum particle breakage. Fig. 4 shows a set of representative scanning electron micrographs with varying cenosphere contents. These figures show that cenospheres are uniformly distributed in syntactic foam structures and no agglomerations are observed in these micrographs. The experimentally measured and theoretically calculated densities of syntactic foams are listed in Table 2. The density of syntactic foams decreases with increasing cenosphere content and becomes 16 % lower for syntactic foam containing 60 vol.% cenospheres, as compared to neat epoxy. The matrix void content increases in a narrow range ($\leq$ 2.6 %) with increasing cenosphere loadings in epoxy resin, as observed from Table 2. The lower matrix void contents signify the higher quality of the fabricated syntactic foams.

ELASTIC MODULUS MEASUREMENT FROM FREE VIBRATION TESTING

Young's modulus is calculated based on the first natural frequency obtained from the free vibration tests and using the equation from Thomson, Dahleh, and Padmanabhan [28] as follows:

$$\omega_j = \beta_j^2 \sqrt{\frac{EI}{\rho^{exp} AL^4}} \tag{3}$$

$$E = \left(\frac{\omega_j}{\beta_j^2}\right)^2 \left(\frac{\rho^{exp} AL^4}{I}\right) \tag{4}$$

FIG. 4

Scanning electron micrograph of (a) E20, (b) E40, and (c) E60 foam samples.

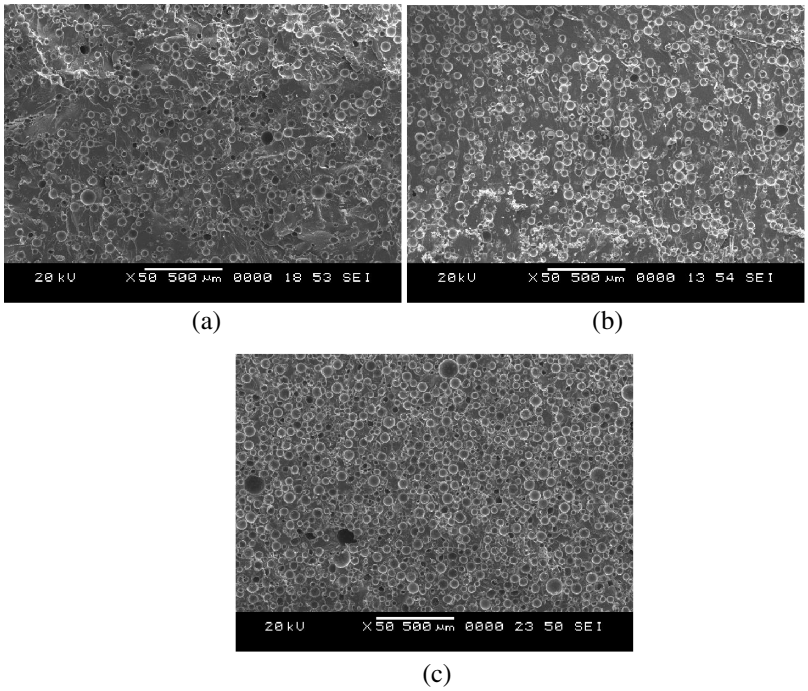

where ω_j is the angular natural frequency ($\omega = 2\pi f$), f is the natural frequency obtained from the free vibration test, E is Young's modulus, and I is the moment of inertia. ρ^{exp} is the experimental density of syntactic foams, and A is the cross-sectional area.

The Bardella-Genna model [29] is utilized to estimate the syntactic foam modulus through a theoretical approach, which is used to compare to experimental values. This model correlates the predicted modulus with microstructural parameters such as radius ratio and wall thickness. A homogenization scheme is used in this model to predict the bulk and shear moduli [29]. See the following:

$$K = K_m \frac{\delta(1+\phi) + \kappa(1+\phi)\gamma}{\delta(1-\phi) + \kappa(\gamma+\phi)} \tag{5}$$

where $\gamma = \frac{4G_m}{3K_m}$, $\delta = \frac{4G_i}{3K_m}(1-\eta^3)$, and $\kappa = \frac{4G_i}{3K_i} + \eta^3$, and η is the radius ratio; K and G are the bulk and shear moduli; subscripts 'm' and 'i' represent the matrix and inclusions, respectively; and ϕ designates the volume fraction of filler. The full expression for the shear modulus is lengthy and can be found in Ref. [29].

The radius ratio (η) is defined as the ratio of the internal radius to the outer radius of cenospheres. The radius ratio increases with decreases in wall thickness and is used in the model to define the geometry of the particle in conjunction with the particle radius [29]. As observed from **Fig. 3**, sphericity variations, porosity within the cenospheres' shells, and variations in the wall thickness make it difficult to predict the radius ratio. Hence, the effective radius ratio is calculated based on the true particle density (ρ_f) and measured density of the cenosphere wall material ($\rho_{ceramic}$) [9] as follows:

$$\eta = \left(1 - \frac{\rho_f}{\rho_{ceramic}}\right)^{\frac{1}{3}} \tag{6}$$

Considering the major constituents of the cenospheres, SiO_2 and Al_2O_3, whose densities are 2,650 and 3,950 kg/m^3, respectively [9], using the weighted composition, the density of the cenosphere wall material is found to be 3,065 kg/m^3 ($\rho_{ceramic}$). ρ_f is taken as 920 kg/m^3 (see **Table 1**). The radius ratio of the cenospheres is found to be 0.8878 ~ 0.9. In the next step, the curve fitting method is used to obtain the cenosphere modulus (keeping $\eta \approx 0.9$) that provides predictions close to the experimental values. Thereby, Young's modulus of cenospheres is found to be 73 GPa, which is used to calculate the syntactic foams modulus in the next steps. Poisson's ratio of the cenospheres is assumed to be 0.2 [9]. The modulus of the matrix is obtained from the free vibration test as 3,920 MPa (see **Table 3**). Poisson's ratio of epoxy resin is 0.35 [30]. Finally, the elastic modulus of foam is given by the following:

TABLE 3
Comparison of experimentally measured and theoretically calculated Young's modulus for syntactic foams.

	Young's Modulus, MPa		
Material Type	Free Vibration	Bardella-Genna Model	% Difference
E0	3,917.81 ± 94.03	3,917.81	0
E20	4,448.54 ± 80.07	4,541.20	−2.08
E40	5,380.43 ± 96.84	5,258.30	2.27
E60	5,848.68 ± 70.18	6,100.40	−4.30

$$E = \frac{9KG}{3K + G} \tag{7}$$

Table 3 represents Young's modulus of syntactic foams, calculated using the Bardella-Genna model. Deviations in the theoretical results from the experimental results are attributed to the defects present in the cenosphere shells.

CRITICAL BUCKLING LOAD ESTIMATIONS

The buckling load shows an increasing trend as a function of filler content (see Fig. 5). The maximum P_{cr} is measured as 387.33 N for E60, which is 63 % higher as compared to neat resin (see Table 4). The increase in the buckling load is in the range of 20–63 % and 21–64 % using DTM and MBC approaches, respectively, with an increasing filler volume fraction. This trend is attributed to the observation that cenospheres have a higher modulus than the matrix resin. The DTM estimates of P_{cr} are higher than those from MBC, although the difference between them is only 1–3 %.

The theoretical critical buckling load is calculated using the Euler buckling formula for clamped-clamped boundary conditions [31] and is given by the following:

$$P_{cr} = \frac{4\pi^2 EI}{L^2} \tag{8}$$

FIG. 5

A representative set of graphs showing experimental buckling behavior of neat epoxy and syntactic foams.

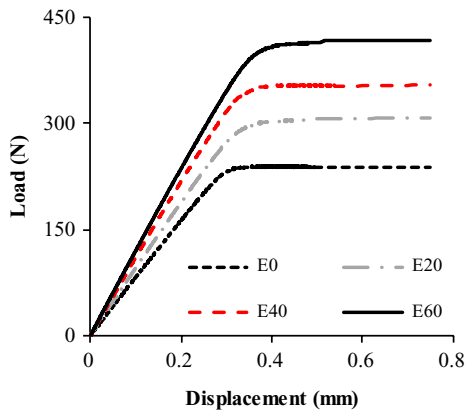

TABLE 4

Critical buckling loads by DTM and MBC for syntactic foams.

Material Type	P_{cr}, N		% Increase in P_{cr} in Syntactic Foams for DTM
	DTM	MBC	
E0	238.50 ± 11.02	231.33 ± 12.51	–
E20	287.58 ± 12.35	281.83 ± 12.85	20.58
E40	343.45 ± 14.29	339.33 ± 14.36	44.00
E60	387.33 ± 15.04	379.17 ± 17.03	62.40

TABLE 5
Comparison of critical buckling loads for syntactic foams.

	P_{cr}, N		
Material Type	Experimental (MBC)	Theoretical	% Difference
E0	231.33 ± 12.51	233.88	−0.88
E20	281.83 ± 12.85	271.08	3.81
E40	339.33 ± 14.36	313.89	7.50
E60	379.17 ± 17.03	364.16	3.96

Table 5 shows a comparison between the experimental and theoretical buckling loads, which are found to be in good agreement for all the specimens. Deviation from the expected values might be due to particle-to-particle interactions resulting in cenosphere breakage during material fabrication. Such models can guide the development of syntactic foams as per the requirements of an application.

FREE VIBRATION UNDER NO LOAD CONDITION AND AXIAL COMPRESSIVE LOADS

Frequency response functions are used to estimate the natural frequency of the syntactic foams. Fig. 6 presents the frequency response functions, which are used to find the natural frequencies corresponding to the first three bending mode shapes. The influence of the cenosphere volume fraction on the natural frequencies of the syntactic foams at no load condition is listed in Table 6. The natural frequency of the syntactic foams increases with the cenosphere volume fraction. The increase in the natural frequencies of the syntactic foams is attributed to the increase in the overall stiffness of the composite due to the addition of stiffer cenospheres.

Furthermore, the natural frequencies of all the syntactic foams are measured at 50 N load increments in the clamped-clamped configuration. Loading is continued until the load plateau is reached. Increasing the compressive load decreases the natural frequencies of all the tested samples corresponding to the first three bending mode shapes (see Fig. 7). Such a reduction in the first fundamental frequency continues until the appearance of the

FIG. 6
Frequency response functions of representative neat epoxy and syntactic foams.

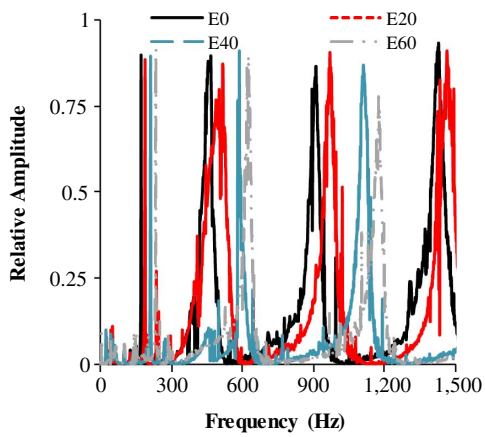

TABLE 6
Free vibration frequency of neat epoxy and their syntactic foams at no load condition.

	Experimental Frequency, Hz		
Material Type	Mode 1	Mode 2	Mode 3
E0	169.18 ± 2.26	463.65 ± 2.89	938.25 ± 4.24
E20	186.37 ± 14.72	516.53 ± 14.14	1,001.00 ± 12.94
E40	210.25 ± 3.74	587.17 ± 7.71	1,145.00 ± 15.55
E60	225.28 ± 7.61	611.26 ± 8.42	1,188.30 ± 9.97
	Theoretical Frequency, Hz		
Material Type	Mode 1	Mode 2	Mode 3
E0	169.18	466.36	914.24
E20	186.42	513.87	1,007.39
E40	209.07	576.31	1,129.80
E60	221.38	610.25	1,196.34

FIG. 7 Natural frequency as a function of increasing load for (a) Mode 1, (b) Mode 2, and (c) Mode 3 for neat epoxy and syntactic foams.

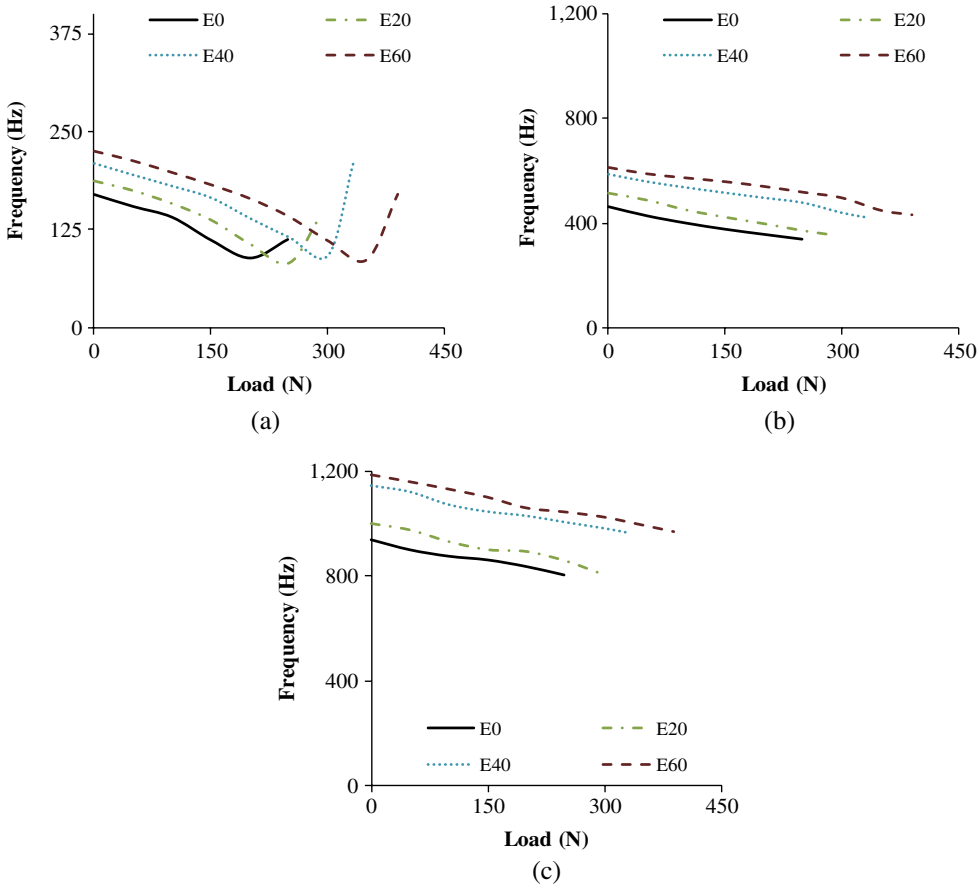

critical buckling point and later starts increasing for all the compositions. This is because the stiffness increases because of the change in the geometry of the sample from linearity to a buckled shape. The natural frequency increases with the filler content under the applied loads, similar to the no-load conditions as observed earlier.

VIBRATION CORRELATION TECHNIQUE

VCT is a nondestructive test used to compute P_{cr} from the vibration data [32–36]. The accuracy of the method depends on how well the technique is able to estimate P_{cr} using data that correspond to the lower levels of the compressive loadings. VCT involves applying compressive load below P_{cr} and evaluating the natural frequency. The procedure is repeated for multiple loading steps. In the present work, the frequency squared-load is plotted up to 200 N and extrapolated to get P_{cr} using a second-order polynomial expression obtained based on the expression in Ref. [37] and is given by the following:

$$\left(\frac{f}{f_n}\right)^2 = 1 - \left(\frac{P}{P_{cr}}\right) \tag{9}$$

FIG. 8

P_{cr} using VCT for neat epoxy and their syntactic foams in Mode 1.

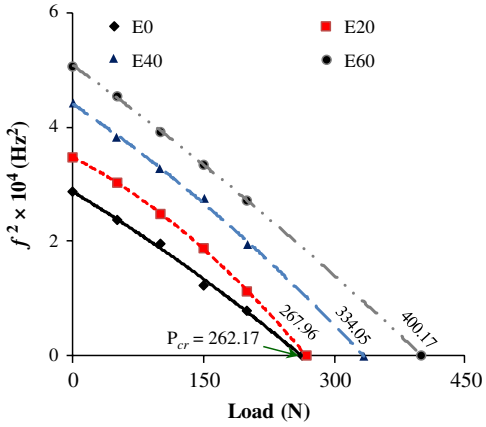

FIG. 9

Buckling load comparison between VCT and experimental approaches.

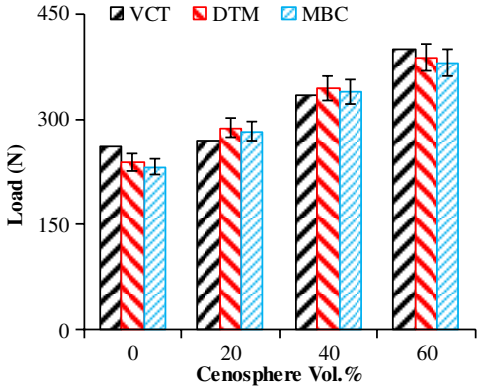

where f_n and f are the fundamental frequencies at no load condition and under compressive load P, respectively. Fig. 8 shows a variation of the frequency squared values as a function of load. The P_{cr} predicted for each configuration through VCT is marked. The VCT-predicted buckling load increases with the volume fraction of the cenosphere, as observed in the buckling experiments. The critical buckling loads predicted through various techniques for the different volume fractions of the cenospheres are compared in Fig. 9. Mixed trends are observed from the comparative results perspective. VCT overpredicted the buckling loads for the E0 and E60 samples but underpredicted for E20 and E40. However, in all the cases, the difference is less than 10 %.

Conclusions

An experimental study is carried out on cenosphere/epoxy syntactic foams to investigate the effect of the particle volume fraction on the buckling load and free vibration characteristics. The critical buckling load increases with the cenosphere volume fraction. Theoretically calculated buckling loads are in good agreement with the experimental results. The natural frequency increases with the cenosphere volume fraction but decreases as the axial load increases. A distinct trend in the natural frequency with an increase in the axial load is observed in the post-buckling regime. The fundamental frequency reaches the lowest value around the buckling load and increases rapidly in the post-buckling region.

ACKNOWLEDGMENTS

Author Nikhil Gupta acknowledges the Office of Naval Research Grant N00014-10-1-0988. International Travel Support by TEQIP-II, NIT-K for the Research Interaction at Composite Materials and Mechanics Laboratory at NYU is acknowledged by P. Jeyaraj. Mrityunjay Doddamani acknowledges the Department of Science and Technology Grant DST/TSG/AMT/2015/394/G. The authors thank the ME Department at NIT-K and the MAE Department at NYU for providing facilities and support. Steven E. Zeltmann is thanked for help in the manuscript preparation.

References

[1] Manakari, V., Parande, G., Doddamani, M., Gaitonde, V. N., Siddhalingeshwar, I. G., Kishore, Shunmugasamy, V. C., and Gupta, N., "Dry Sliding Wear of Epoxy/Cenosphere Syntactic Foams," *Tribol. Int.*, Vol. 92, 2015, pp. 425–438, https://doi.org/10.1016/j.triboint.2015.07.026

[2] Gupta, N., Zeltmann, S. E., Shunmugasamy, V. C., and Pinisetty, D., "Applications of Polymer Matrix Syntactic Foams," *JOM*, Vol. 66, No. 2, 2014, pp. 245–254, https://doi.org/10.1007/s11837-013-0796-8

[3] Gu, J., Wu, G., and Zhao, X., "Effect of Surface-Modification on the Dynamic Behaviors of Fly Ash Cenospheres Filled Epoxy Composites," *Polym. Compos.*, Vol. 30, No. 2, 2009, pp. 232–238, https://doi.org/10.1002/pc.20562

[4] Gupta, N., Ye, R., and Porfiri, M., "Comparison of Tensile and Compressive Characteristics of Vinyl Ester/Glass Microballoon Syntactic Foams," *Compos. Part B: Eng.*, Vol. 41, No. 3, 2010, pp. 236–245, https://doi.org/10.1016/j.compositesb.2009.07.004

[5] Bardella, L., Malanca, F., Ponzo, P., Panteghini, A., and Porfiri, M., "A Micromechanical Model for Quasi-Brittle Compressive Failure of Glass-Microballoons/Thermoset-Matrix Syntactic Foams," *J. Eur. Ceram. Soc.*, Vol. 34, No. 11, 2014, pp. 2605–2616, https://doi.org/10.1016/j.jeurceramsoc.2013.11.045

[6] Gupta, N., Woldesenbet, E., and Mensah, P., "Compression Properties of Syntactic Foams: Effect of Cenosphere Radius Ratio and Specimen Aspect Ratio," *Compos. Part A: Appl. Sci. Manuf.*, Vol. 35, No. 1, 2004, pp. 103–111, https://doi.org/10.1016/j.compositesa.2003.08.001

[7] Yu, M., Zhu, P., and Ma, Y., "Global Sensitivity Analysis for the Elastic Properties of Hollow Spheres Filled Syntactic Foams Using High Dimensional Model Representation Method," *Comput. Mater. Sci.*, Vol. 61, 2012, pp. 89–98, https://doi.org/10.1016/j.commatsci.2012.04.005

[8] Doddamani, M., Kishore, Shunmugasamy, V. C., Gupta, N., and Vijayakumar, H. B., "Compressive and Flexural Properties of Functionally Graded Fly Ash Cenosphere–Epoxy Resin Syntactic Foams," *Polym. Compos.*, Vol. 36, No. 4, 2015, pp. 685–693, https://doi.org/10.1002/pc.22987

[9] Labella, M., Zeltmann, S. E., Shunmugasamy, V. C., Gupta, N., and Rohatgi, P. K., "Mechanical and Thermal Properties of Fly Ash/Vinyl Ester Syntactic Foams," *Fuel*, Vol. 121, 2014, pp. 240–249, https://doi.org/10.1016/j.fuel.2013.12.038

[10] Pinisetty, D., Shunmugasamy, V. C., and Gupta, N., "6 - Hollow Glass Microspheres in Thermosets—Epoxy Syntactic Foams," *Hollow Glass Microspheres for Plastics, Elastomers, and Adhesives Compounds*, William Andrew Publishing, Norwich, NY, 2015, pp. 147–174.

[11] Gupta, N., Gupta, S. K., and Mueller, B. J., "Analysis of a Functionally Graded Particulate Composite under Flexural Loading Conditions," *Mater. Sci. Eng.: A*, Vol. 485, Nos. 1–2, 2008, pp. 439–447, https://doi.org/10.1016/j.msea.2007.08.020

[12] Zhu, B., Ma, J., Wang, J., Wu, J., and Peng, D., "Thermal, Dielectric and Compressive Properties of Hollow Glass Microsphere Filled Epoxy-Matrix Composites," *J. Reinf. Plast. Compos.*, Vol. 31, No. 19, 2012, pp. 1311–1326, https://doi.org/10.1177/0731684412452918

[13] Yung, K. C., Zhu, B. L., Yue, T. M., and Xie, C. S., "Preparation and Properties of Hollow Glass Microsphere-Filled Epoxy-Matrix Composites," *Compos. Sci. Technol.*, Vol. 69, No. 2, 2009, pp. 260–264, https://doi.org/10.1016/j.compscitech.2008.10.014

[14] Shams, A., Aureli, M., and Porfiri, M., "Nonlinear Buckling of a Spherical Shell Embedded in an Elastic Medium with Imperfect Interface," *Int. J. Solids Struct.*, Vol. 50, Nos. 14–15, 2013, pp. 2310–2327, https://doi.org/10.1016/j.ijsolstr.2013.03.020

[15] Huang, R., Li, P., Wang, Z., and Liu, T., "X-Ray Microtomographic Characterization and Quantification of the Strain Rate Dependent Failure Mechanism in Cenosphere Epoxy Syntactic Foams," *Adv. Eng. Mater.*, Vol. 18, No. 9, 2016, pp. 1550–1555, https://doi.org/10.1002/adem.201600215

[16] Matsunaga, H., "Free Vibration and Stability of Thin Elastic Beams Subjected to Axial Forces," *J. Sound Vibr.*, Vol. 191, No. 5, 1996, pp. 917–933, https://doi.org/10.1006/jsvi.1996.0163

[17] Matsunaga, H., "Buckling Instabilities of Thick Elastic Beams Subjected to Axial Stresses," *Comput. Struct.*, Vol. 59, No. 5, 1996, pp. 859–868, https://doi.org/10.1016/0045-7949(95)00306-1

[18] Zhu, S., Yan, J., Chen, Z., Tong, M., and Wang, Y., "Effect of the Stiffener Stiffness on the Buckling and Post-Buckling Behavior of Stiffened Composite Panels – Experimental Investigation," *Compos. Struct.*, Vol. 120, 2015, pp. 334–345, https://doi.org/10.1016/j.compstruct.2014.10.021

[19] Yeter, E., Erkliğ, A., and Bulut, M., "Hybridization Effects on the Buckling Behavior of Laminated Composite Plates," *Compos. Struct.*, Vol. 118, 2014, pp. 19–27, https://doi.org/10.1016/j.compstruct.2014.07.020

[20] Yang, J., Wu, H., and Kitipornchai, S., "Buckling and Postbuckling of Functionally Graded Multilayer Graphene Platelet-Reinforced Composite Beams," *Compos. Struct.*, Vol. 161, 2017, pp. 111–118, https://doi.org/10.1016/j.compstruct.2016.11.048

[21] Lamanna, E., Gupta, N., Cappa, P., Strbik, O. M., III, and Cho, K., "Evaluation of the Dynamic Properties of an Aluminum Syntactic Foam Core Sandwich," *J. Alloys Compd.*, Vol. 695, 2017, pp. 2987–2994, https://doi.org/10.1016/j.jallcom.2016.11.361

[22] Malik, P. and Kadoli, R., "Thermo-Elastic Response of SUS316-Al2O3 Functionally Graded Beams under Various Heat Loads," *Int. J. Mech. Sci.*, Vols. 128–129, 2017, pp. 206–223, https://doi.org/10.1016/j.ijmecsci.2017.04.014
[23] Nagendra Gopal, K. V. and Asdev, J., "Dynamic Response of Syntactic Foam Core Sandwich Using a Multiphase Scales Based Asymtotic Method," presented at the *16th European Conference on Composite Materials (ECCM-16)*, Seville, Spain, June 22–26, 2014, European Society for Composite Materials, Wels, Austria.
[24] Jun, L., Li, J., and Xiaobin, L., "A Spectral Element Model for Thermal Effect on Vibration and Buckling of Laminated Beams Based on Trigonometric Shear Deformation Theory," *Int. J. Mech. Sci.*, Vol. 133, 2017, pp. 100–111, https://doi.org/10.1016/j.ijmecsci.2017.07.059
[25] Rahmani, O., Khalili, S. M. R., Malekzadeh, K., and Hadavinia, H., "Free Vibration Analysis of Sandwich Structures with a Flexible Functionally Graded Syntactic Core," *Compos. Struct.*, Vol. 91, No. 2, 2009, pp. 229–235, https://doi.org/10.1016/j.compstruct.2009.05.007
[26] Tuttle, M., Singhatanadgid, P., and Hinds, G., "Buckling of Composite Panels Subjected to Biaxial Loading," *Exp. Mech.*, Vol. 39, No. 3, 1999, pp. 191–201, https://doi.org/10.1007/BF02323552
[27] Shariyat, M., "Thermal Buckling Analysis of Rectangular Composite Plates with Temperature-Dependent Properties Based on a Layerwise Theory," *Thin-Walled Struct.*, Vol. 45, No. 4, 2007, pp. 439–452, https://doi.org/10.1016/j.tws.2007.03.004
[28] Thomson, W. T., Dahleh, M. D., and Padmanabhan, C., *Theory of Vibrations with Applications*, 5th ed., Pearson Education, London, UK, 2008, pp. 268–300.
[29] Bardella, L. and Genna, F., "On the Elastic Behavior of Syntactic Foams," *Int. J. Solids Struct.*, Vol. 38, Nos. 40–41, 2001, pp. 7235–7260, https://doi.org/10.1016/S0020-7683(00)00228-6
[30] Shams, A. and Porfiri, M., "A Generalized Vlasov-Jones Foundation Model for Micromechanics Studies of Syntactic Foams," *Compos. Struct.*, Vol. 103, 2013, pp. 168–178, https://doi.org/10.1016/j.compstruct.2013.04.020
[31] Jones, R., *Buckling of Bars, Plates and Shells*, Taylor & Francis Incorporated, Hoboken, NJ, 1999, pp. 49–226.
[32] Abramovich, H., Govich, D., and Grunwald, A., "Buckling Prediction of Panels Using the Vibration Correlation Technique," *Prog. Aerosp. Sci.*, Vol. 78, 2015, pp. 62–73, https://doi.org/10.1016/j.paerosci.2015.05.010
[33] Plaut, R. H. and Virgin, L. N., "Use of Frequency Data to Predict Buckling," *J. Eng. Mech.*, Vol. 116, No. 10, 1990, pp. 2330–2335, https://doi.org/10.1061/(ASCE)0733-9399(1990)116:10(2330)
[34] Arbelo, M. A., de Almeida, S. F. M., Donadon, M. V., Rett, S. R., Degenhardt, R., Castro, S. G. P., Kalnins, K., and Ozoliņš, O., "Vibration Correlation Technique for the Estimation of Real Boundary Conditions and Buckling Load of Unstiffened Plates and Cylindrical Shells," *Thin-Walled Struct.*, Vol. 79, 2014, pp. 119–128, https://doi.org/10.1016/j.tws.2014.02.006
[35] Arbelo, M. A., Kalnins, K., Ozolins, O., Skukis, E., Castro, S. G. P., and Degenhardt, R., "Experimental and Numerical Estimation of Buckling Load on Unstiffened Cylindrical Shells Using a Vibration Correlation Technique," *Thin-Walled Struct.*, Vol. 94, 2015, pp. 273–279, https://doi.org/10.1016/j.tws.2015.04.024
[36] Souza, M. A. and Assaid, L. M. B., "A New Technique for the Prediction of Buckling Loads from Nondestructive Vibration Tests," *Exp. Mech.*, Vol. 31, No. 2, 1991, pp. 93–97, https://doi.org/10.1007/BF02327558
[37] Jia, J., *Essentials of Applied Dynamic Analysis (Risk Engineering)*, Springer, New York, NY, 2014, 424p.